



RESEARCH LETTER

10.1002/2015GL063911

Key Points:

- Decadal variability of western Amazon dry-season hydroclimate is quantified
- Atlantic and Amazon decadal covariability is well reproduced in CMIP5 models
- Current Atlantic decadal phase favors drier dry seasons in western Amazon

Supporting Information:

- Figure S1

Correspondence to:

K. Fernandes,
katia@iri.columbia.edu

Citation:

Fernandes, K., A. Giannini, L. Verchot, W. Baethgen, and M. Pinedo-Vasquez (2015), Decadal covariability of Atlantic SSTs and western Amazon dry-season hydroclimate in observations and CMIP5 simulations, *Geophys. Res. Lett.*, **42**, doi:10.1002/2015GL063911.

Received 19 MAR 2015

Accepted 4 MAY 2015

Accepted article online 8 MAY 2015

Decadal covariability of Atlantic SSTs and western Amazon dry-season hydroclimate in observations and CMIP5 simulations

Katia Fernandes^{1,2}, Alessandra Giannini¹, Louis Verchot², Walter Baethgen¹, and Miguel Pinedo-Vasquez^{2,3}

¹International Research Institute for Climate and Society, Columbia University, Palisades, New York, USA, ²Center for International Forestry Research, Bogor, Indonesia, ³Earth Institute Center for Environmental Sustainability, Columbia University, New York, New York, USA

Abstract The unusual severity and return time of the 2005 and 2010 dry-season droughts in western Amazon is attributed partly to decadal climate fluctuations and a modest drying trend. Decadal variability of western Amazon hydroclimate is highly correlated to the Atlantic sea surface temperature (SST) north-south gradient (NSG). Shifts of dry and wet events frequencies are also related to the NSG phase, with a 66% chance of 3+ years of dry events per decade when NSG > 0 and 19% when NSG < 0. The western Amazon and NSG decadal covariability is well reproduced in general circulation models (GCMs) historical (HIST) and preindustrial control (PIC) experiments of the Coupled Model Intercomparison Project Phase 5 (CMIP5). The HIST and PIC also reproduce the shifts in dry and wet events probabilities, indicating potential for decadal predictability based on GCMs. Persistence of the current NSG positive phase favors above normal frequency of western Amazon dry events in coming decades.

1. Introduction

The drought of 2005 was a “1 in 100 years” event in western Amazon resulting in fire damage to over 300,000 ha of rainforest and over US\$ 50 million in losses [Brown *et al.*, 2006]. Five years later, an even more severe drought isolated entire floodplain communities due to unprecedented low river levels [Marengo *et al.*, 2011]. The Amazon ecosystem is sensitive to repeated occurrence of droughts, which interferes with the forest’s natural ability to recover from stress [da Costa *et al.*, 2010; Saatchi *et al.*, 2013] and undermines climate change mitigation efforts to reduce CO₂ emissions from deforestation and forest degradation [Aragão and Shimabukuro, 2010]. Whether the unusual severity of recent droughts is related to natural low-frequency modes of climate variability, to long-term climate trends, or to their combination is explored here.

Historical trends in the Amazon’s precipitation have been reported in literature and vary considerably among studies depending on the data set, time series period and length, season, and Amazon region evaluated [Costa and Foley, 1999; Li *et al.*, 2008; Malhi and Wright, 2004; Marengo, 2009; Villar *et al.*, 2009]. This highly variable character of trends is also seen in general circulation model (GCM) simulations of the 20th and 21st centuries as models present a large spread among estimates [Joetzer *et al.*, 2013; Li *et al.*, 2008; Orłowsky and Seneviratne, 2013; Stocker *et al.*, 2013]. These discrepancies are attributed partly to the lack of consensus on the patterns and magnitude of SST anomalies in the models [Good *et al.*, 2008, 2009; Joetzer *et al.*, 2013]. Significant climate fluctuations on decadal time scale could also explain acceleration or deceleration of trends calculated over periods shorter than the full decadal cycle [DelSole *et al.*, 2011]. Decadal changes in the Amazon precipitation regime have been attributed to phase shifts of the Pacific Decadal Oscillation and Atlantic Multidecadal Oscillation (AMO) [Kayano *et al.*, 2009; Marengo, 2009; Villar *et al.*, 2009]. Yet no systematic analysis has been conducted to quantify the importance of decadal fluctuations to dry-season variability or whether decadal covariability of SSTs and western Amazon precipitation anomalies are well reproduced in GCMs. In West Africa where the role of SST as the driver of rainfall decadal variability is better understood [Folland *et al.*, 1986; Giannini *et al.*, 2003; Hastenrath, 1990], the Intergovernmental Panel for Climate Change (IPCC) Coupled Model Intercomparison Project Phase 5 (CMIP5) GCMs [Taylor *et al.*, 2012] are able to reproduce main SST and rainfall teleconnections [Giannini *et al.*, 2013; Martin *et al.*, 2014].

Where decadal fluctuations explain a significant portion of total variability, models must be able to reproduce the related physical processes if we expect them to produce skillful simulations of the current and future climate. Hence, our objectives are (i) to quantify the portion of the western Amazon dry-season hydroclimate variability that is related to decadal fluctuations and this is accomplished by statistically partitioning the time series into trend, decadal, and interannual time scales; (ii) to determine the main large-scale ocean patterns related to the decadal fluctuations of western Amazon dry-season climate using linear regression analysis; (iii) to investigate whether observed coupling of large-scale processes and western Amazon precipitation are reproduced in CMIP5 GCMs; and (iv) to explore the potential for probabilistic decadal prediction of frequency of dry and wet events.

2. Data and Methods

2.1. Observational Data

The driest season in western Amazon is JAS (July, August, and September), for which a 3 month Standardized Precipitation Index (SPI) [McKee *et al.*, 1993] is calculated. SPI is the number of standard deviations that the observed cumulative precipitation deviates from climatology and can be used to assess equally positive and negative anomalies, requiring only precipitation for its calculation. It is also the meteorological drought index recommended by the World Meteorological Organization [Svoboda *et al.*, 2012]. The Global Precipitation Climatology Centre (GPCC) (version 6) rain-gauge-only data set is used at $0.5^\circ \times 0.5^\circ$ spatial resolution and monthly time steps from 1935 to 2010 [Schneider *et al.*, 2014]. The period through 2012 is complemented by GPCC First Guess product [Schamm *et al.*, 2014]. The JAS-SPI is derived from averaged precipitation over the western Amazon domain (16°S – 2°N and 76.5°W – 60.5°W), which is defined to represent a common area of the 2005 and 2010 droughts. Grid points outside the Amazon River basin are excluded from calculations. The JAS-SPI time series analysis is complemented with river level data from the Rio Negro (RNWL), an Amazon western tributary, reporting continuous records since the early 1900s. The RNWL provides an integrated measure of basin precipitation that does not depend on rain gauges density upstream. We calculate standardized anomalies of the minimum water level value observed between 1 October and 31 December, which is the period when dry-season precipitation anomalies would reflect on the river level [ANA, 2014]. The western Amazon domain JAS-SPI variability is not substantially affected by the number of reporting stations during the 1935–2012 period, as 20 years running correlations between JAS-SPI and RNWL remain statistically significant over time ($R > 0.57$, $P < 0.01$, $df = 18$).

SST data are obtained from the National Oceanic and Atmospheric Administration (NOAA) Extended Reconstructed Sea Surface Temperature Dataset version 3b (ERSSTv3b) [Smith *et al.*, 2008]. Monthly SST anomaly fields are averaged for April through September (AMJJAS) as precipitation in the Amazon shows concurrent and lagged responses to SST forcings [Fernandes *et al.*, 2011; Yoon and Zeng, 2010] (Figure S1 in the supporting information). We define an AMJJAS Atlantic SST north-south gradient (NSG) index by subtracting the southern (45°W – 0°W , 30°S – 10°S) from the northern (75°W – 10°W , 5°N – 30°N) domain-averaged SST anomalies. The variability of NSG is compared to that of the Atlantic Multidecadal Oscillation (AMO) index [Enfield *et al.*, 2001] obtained from the NOAA-Earth System Research Laboratory (<http://www.esrl.noaa.gov/psd/data/timeseries/AMO/>).

2.2. CMIP5 Experiments

The western Amazon JAS-SPI and SSTs covariability is analyzed in two of the IPCC CMIP5 GCM experiments [Taylor *et al.*, 2012]: the historical (HIST), which are forced with observed atmospheric composition changes from both anthropogenic and natural sources; and the preindustrial control (PIC) with atmospheric composition fixed at preindustrial levels. The longest period common to the HIST experiment's 44 models is 1861–2005. The number of ensemble members varies from one (18 models) to 10 (3 models) totaling 128 HIST ensemble members. The longest common time series for PIC runs consists of 199 years with start and end years varying among models. One ensemble member from each of the 42 PIC models is used. All models are linearly interpolated to a $1^\circ \times 1^\circ$ resolution. Total precipitation is used to calculate western Amazon JAS-SPI and temperature at the Earth's surface (ts), with land areas masked out, represents SST. Prior to averaging over the April to September (AMJJAS), each ensemble member's monthly SST anomaly field is calculated by removing the entire series climatology (145 years for HIST and 199 years for PIC) at each grid point.

The time series partitioning into trend, decadal, and interannual variability consists of first calculating a multimodel, nearly global (60°S–60°N) domain-averaged surface temperature (t_s) from the first ensemble member of the 44 HIST (1861–2005) GCMs [Greene *et al.*, 2011]. We extend the t_s time series to 2012, using the first ensemble member of 27 RCP4.5 GCMs. Globally averaged multimodel mean t_s has an undistinguishable rate of change among various pathways during the first decade of projections [Knutti and Sedlacek, 2013]; thus, we choose the RCP4.5 as it represents a medium-level representative concentration pathway (RCP) mitigation scenario with an approximate target radiative forcing of 4.5 W m^{-2} by 2100 relative to preindustrial conditions [Taylor *et al.*, 2012]. The resulting HIST+RCP4.5 multimodel mean t_s (1861–2012) overlaps entirely the observational period and is smoothed using a 50 year cutoff low-pass Butterworth filter to represent the externally forced warming trend. The observed data (JAS-SPI, RNWL, and NSG) and HIST experiment GCM variables (JAS-SPI and NSG) are regressed on the smoothed t_s time series: the fitted values represent the climate variability linearly related to the GCM's estimated external forcing. This approach assumes that local trends are related to global temperature increase only and local factors (e.g., land-use change) cannot be separated. However, local effects are reduced for area-integrated or area-averaged variables such as the time series partitioned (JAS-SPI, RNWL, and NSG). This method has the advantage of not assuming changes at a constant rate over time but rather as response physical mechanisms related to global temperature changes. The residual of the regression is filtered using a 10 year cutoff low-pass Butterworth filter to retain modes on the scale of decades. The interannual component results from subtracting the external forcing and decadal mode from the original series. The same analysis is conducted for the PIC 42 models using the first 199 years of simulations, except that the multimodel global t_s does not represent an externally forced trend as greenhouse gases (GHG) are fixed at the preindustrial level.

2.3. Linear Regression Analysis

Observed Atlantic and Pacific AMJJAS SST fields are linearly regressed on the decadal components of JAS-SPI and RNWL. The two resulting regression coefficient (RC) fields are averaged for values significant at the 95% level or above (t statistic).

The same analysis is performed on each individual HIST and PIC ensemble member. The regression fields are averaged among HIST models with multiple-ensemble members resulting in one RC field per model. We use model JAS-SPI only, as river level is not a variable available in the models. The HIST and PIC results are presented as multimodel means, and consistency is evaluated by the ratio between the absolute value of the multimodel regression mean and intermodel standard deviation; values greater (lower) than 1 indicate a high (low) level of agreement between models [Meehl *et al.*, 2007].

2.4. Frequency of Dry and Wet Events

Frequency of dry and wet events is evaluated by defining “dry” and “wet” as values equal or below -0.68 and equal or above 0.68 , respectively, for JAS-SPI and RNWL. Both variables follow a Gaussian distribution; thus, the defined thresholds represent the 25% driest and 25% wettest events. If they were distributed uniformly over time, 2.5 dry and 2.5 wet events per decade would be observed. The decadal variation of events frequency is evaluated by counting the occurrences of “dry” and “wet” in 10 year moving windows, using both JAS-SPI and the standardized minimum RNWL time series. The two data sets' average count is assigned to the center of the window period, which results in the year 1940 representing anomalous events count for 1935–1944, 1941 for 1936–1945, and so on, continuing to 2008 for the events count of 2003–2012.

3. Results

3.1. Variability of Western Amazon Dry-Season Hydroclimate and SSTs

The partitioning of the time series into trend, decadal, and interannual time scales is conducted for the western Amazon domain-averaged JAS-SPI and the standardized minimum RNWL. The correlation between the two unfiltered variables is 0.76 ($P < 0.01$, t test) indicating that the predominant climate over the larger western Amazon domain corresponds well to that of the smaller Rio Negro drainage basin (Figure 2). The time series partitioning reveals that the least portion of the dry-season hydroclimate variability is explained by trends corresponding to 3.3% and nearly 6% for the RNWL and JAS-SPI,

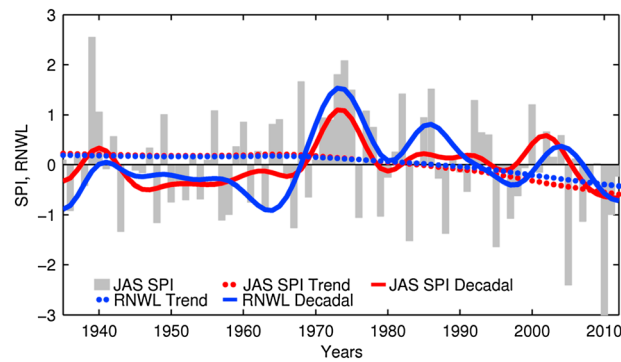


Figure 1. Observed 1935–2012 western Amazon JAS-SPI (grey bars) decomposed into trend (dotted red line) and decadal time scales (solid red line). Trend (dotted blue line) and decadal (solid blue line) components of the standardized minimum RNWL time series are also shown. Standardized units.

Eltahir and Bras, 1994; Fu et al., 2013; Li and Fu, 2004; Marengo, 2009; Salati and Vose, 1984; van der Ent et al., 2010].

Intermediate amounts of total variance are explained by the decadal component of JAS-SPI (16%) and RNWL (32%) as shown in Figure 1. The correlation between the two decadal time series is 0.79, significant at $P < 0.01$, tested using a random-phase method designed for serially correlated time series [Ebisuzaki, 1997]. The decadal oscillation entered a negative phase in the mid-2000s, suggesting that the combined decadal signal and the modest negative trend added to the severity of recent droughts, especially that of 2010.

The decadal time series of JAS-SPI and RNWL (Figure 1) are individually used to calculate regression coefficients with unfiltered Atlantic and Pacific AMJJAS field SST anomalies (Figure 2). The corresponding maps reveal a north-south gradient (NSG) in the Atlantic SST covarying with JAS-SPI and RNWL on decadal time scale. The mechanism linking anomalous NSG in the Atlantic to interannual variability of the Amazon dry-season precipitation has been presented in previous studies. Positive NSG (warmer anomalies in the north relative to the south Atlantic) is associated with a northward migration of the Intertropical Convergence Zone [Cook et al., 2012; Cox et al., 2008; Good et al., 2008] and Atlantic Hadley Cell [Wang, 2002], which results in anomalous subsidence over the Amazon. This is followed by anomalous southerly surface winds over tropical South America, reduced moisture transport from the Atlantic to the Amazon and deficient precipitation, while enhanced moisture transport and abundant precipitation occur in association with the opposite pattern [Yoon and Zeng, 2010].

The regression of HIST SSTs and western Amazon JAS-SPI (Figure 2b) reveal a spatial pattern remarkably similar to that observed, especially in the Atlantic where the RCs multimodel mean is greater than the intermodel standard deviation, indicating consistency among models [Meehl et al., 2007]. Twentieth century multidecadal north Atlantic SST fluctuations have been attributed primarily to internal ocean variability [DelSole et al., 2011; Ting et al., 2009, 2011], to externally forced radiative cooling due to high concentration of anthropogenic aerosol in the Northern Hemisphere [Booth et al., 2012] or a combination of the two [Chang et al., 2011; Terray, 2012; Zhang et al., 2013]. The northern sector of the NSG is significantly correlated with the north Atlantic, namely, the Atlantic Multidecadal Oscillation (AMO) ($R = 0.71$, $P < 0.01$, and t test), while the southern sector is not ($R = 0.11$ and $P < 0.34$). Thus, to evaluate how internal ocean variability compares to external forcings in determining the Atlantic and western Amazon decadal covariability, we regress SSTs on JAS-SPI decadal time series using the PIC simulations for which aerosol and GHG concentrations are fixed at the preindustrial level (Figure 2c).

The spatial distribution of the RCs in the PIC is almost identical to the HIST simulations, revealing consistent patterns of Atlantic and western Amazon precipitation that result from internal processes, regardless of the 20th century influences of GHG or natural and anthropogenic aerosols used to force the HIST simulations. This suggests that decadal fluctuations of western Amazon can occur coupled to ocean internal processes common to both HIST and PIC experiments. The extent to which GHGs and natural and anthropogenic

respectively (Figure 1). Processes on the interannual time scale dominate the variability of JAS-SPI (75%) and RNWL (62%), but this time scale is not addressed here as mechanisms related to the Amazon year-to-year variability have been extensively studied and attributed to atmospheric circulation patterns driven by SST anomalies in the tropical Pacific and Atlantic basins [Fernandes et al., 2011; Fu et al., 2001; Good et al., 2008; Kayano et al., 2009; Marengo, 2009; Parsons et al., 2014; Ropelewski and Halpert, 1987; Yoon and Zeng, 2010; Zeng, 1999] and local land-atmosphere feedbacks [Bosilovich and Chern, 2006; Dirmeyer et al., 2009;

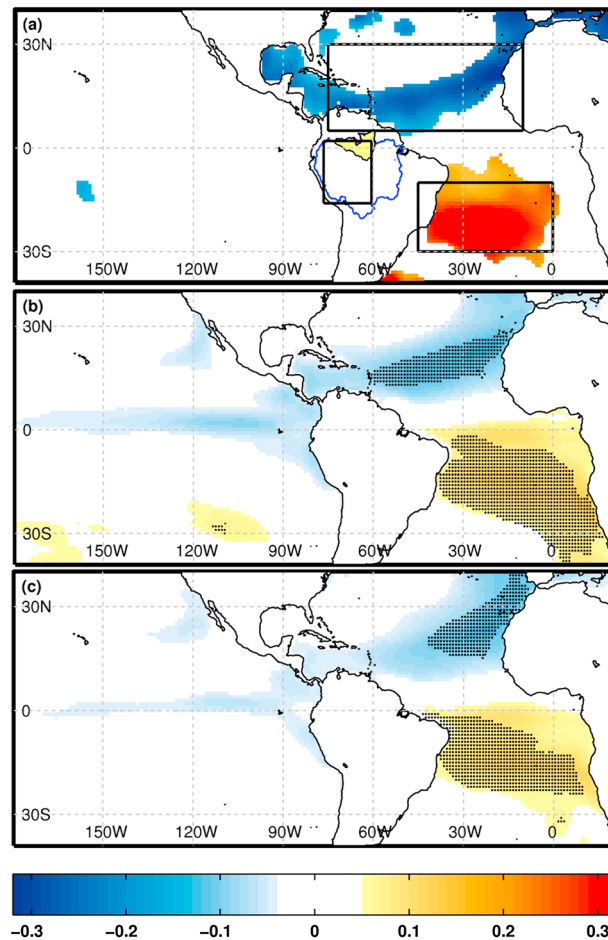


Figure 2. Mean regression coefficients (RCs) of April to September (AMJJAS) SST anomalies ($^{\circ}\text{C}$) on the decadal time series of western Amazon variables. (a) SST regression on JAS-SPI and RNWL (1935–2012). Only 95% significant RCs are averaged. (b) CMIP5 HIST SSTs and JAS-SPI RCs (1861–2005). (c) CMIP5 PIC SSTs and JAS-SPI RCs (199 years). The boxes in Figure 2a represent the western Amazon domain and the north and south Atlantic sectors used to calculate the NSG index. Blue contour and yellow shade in Figure 2a represent the Amazon and Negro river basins, respectively. Stippling in Figures 2b and 2c indicate areas where the multimodel mean values are larger than the intermodel standard deviation, a sign of consistency among models. Unit: $^{\circ}\text{C}$ per standard deviation.

time scale partitioning of the NSG index reveals that 48% of total variance resides on decadal fluctuations (Figure 3), while the trend and interannual components correspond to 1% and 46%, respectively (not shown). The periodicity of the decadal NSG indicates a cycle of multiple decades, in agreement with studies of Atlantic interhemispheric SST gradients [Chang *et al.*, 2011; Chiang *et al.*, 2013; Cox *et al.*, 2008; Kossin and Vimont, 2007; Latif *et al.*, 2006]. The decadal components of JAS-SPI, RNWL (Figure 1) and the NSG index are remarkably synchronized over the period analyzed, as reflected by the correlation between the NSG index and JAS-SPI ($R = -0.88$) and the NSG index and RNWL ($R = -0.84$), both significant at $P < 0.01$ [Ebisuzaki, 1997].

The frequency of dry and wet events also varies according to the decadal phase of the NSG (Figure 3). For each JAS-SPI and RNWL, dry and wet events correspond to the 25% driest and wettest occurrences over the period 1935–2012, or equivalent to an average of 2.5 events per decade. Above average frequency of 3 or more, dry events within a decade were a common occurrence prior to the mid-1960s and then again, although more irregularly, in the 1990s and 2000s, coinciding with the positive phase of the NSG decadal

aerosols project onto this pattern of internal variability and impact Atlantic SSTs, while plausible, remains controversial [Booth *et al.*, 2012; Chiang *et al.*, 2013; Cox *et al.*, 2008; Zhang *et al.*, 2013].

Our findings build on previous work describing interannual covariability of Atlantic SSTs and Amazon dry-season precipitation [Cook *et al.*, 2012; Fernandes *et al.*, 2011; Good *et al.*, 2008; Marengo *et al.*, 2011; Yoon and Zeng, 2010], as it reveals that this relationship is also observed on the scale of decades and it is collectively well reproduced in both HIST and PIC CMIP5 experiments. However, on average, the models underestimate the intensity of the coupling as RC values are lower than those observed. This is likely due to an inadequate representation of the precipitation decadal variability magnitude in GCMs [Ault *et al.*, 2012], which limits the use of models to assess precipitation intensity. Event frequencies show clearer signals than magnitudes in GCMs [Orlowsky and Seneviratne, 2013]; thus, we conduct a complementary analysis to evaluate the probability distribution of event frequencies (dry and wet) by NSG phase in observations and models.

3.2. Decadal Frequency of Dry and Wet Events

The impact of Atlantic decadal fluctuations on the frequency of western Amazon dry and wet dry seasons is evaluated by initially defining an Atlantic SST NSG index. The AMJJAS SST anomalies averaged over the south are subtracted from the north domain (Figure 2a). The

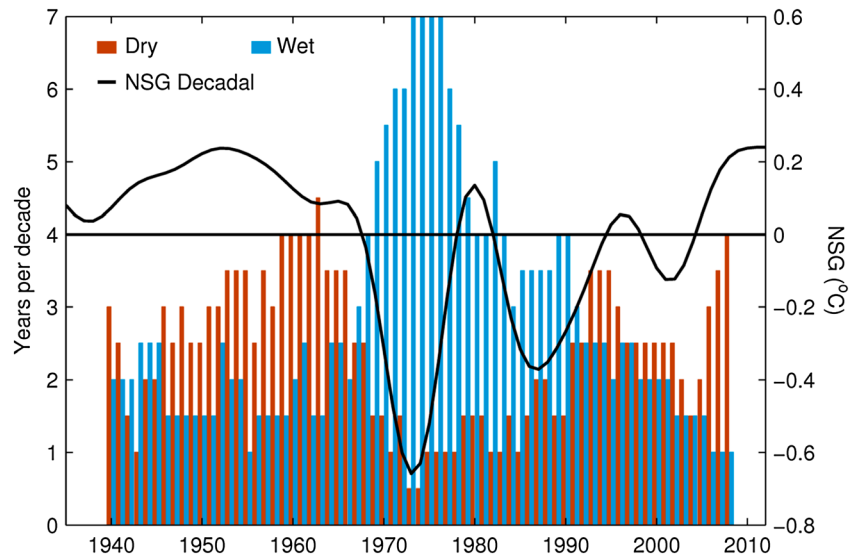


Figure 3. Number of dry-season dry (brown) and wet (blue) events per decade averaged for the JAS-SPI and standardized minimum RNWL counts. Frequencies are calculated for 10 year moving windows and plotted at the center of the window period. Black line is the decadal component of the Atlantic SST north-south gradient (NSG) in unit of °C.

mode. In the 1970s and 1980s at least 3 and as many as 7 years of wet events per decade were observed, concurrent with the NSG negative phase.

This shift in frequency as a function of the NSG decadal phase is also shown as histograms (Figure 4), calculated from JAS-SPI and RNWL dry and wet event counts per decade. The 78 year long time series (1935–2012) results in 69 ten year moving windows samples for each JAS-SPI and RNWL, which are then

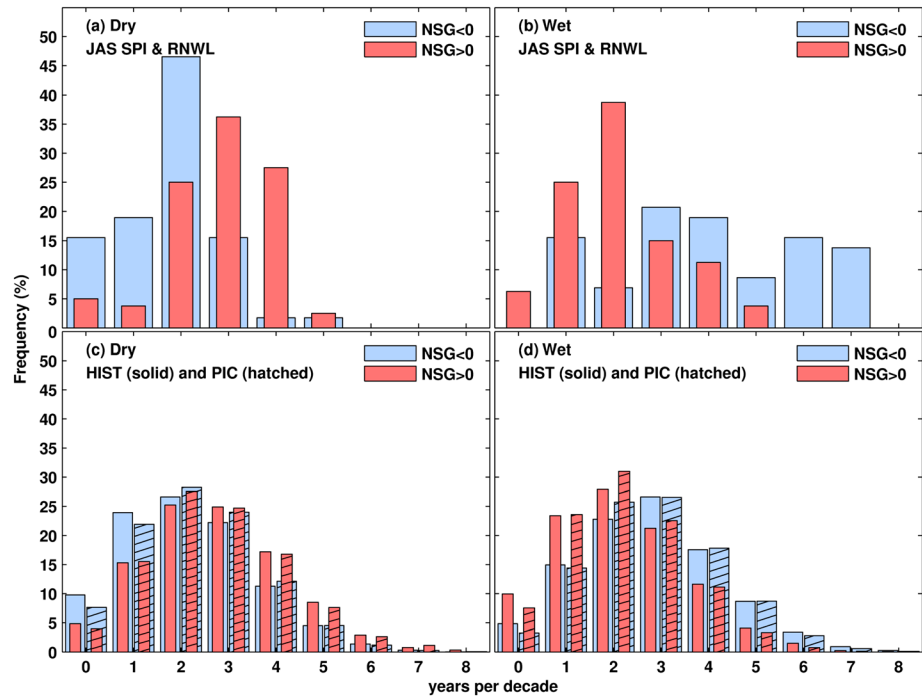


Figure 4. Histograms of 10 year moving windows of (a and c) dry and (b and d) wet events frequencies during positive (pink) and negative (blue) Atlantic NSG phases. Figures 4a and 4b represent observations (JAS-SPI and RNWL) and Figures 4c and 4d the CMIP5 HIST (solid colors) and PIC (hatched) experiments.

grouped according to the NSG index decadal phase. The distributions of JAS-SPI and RNWL dry (Figure 4a) and wet (Figure 4b) frequencies are statistically different ($P < 0.01$, using a two-sample Kolmogorov-Smirnov test [Wilks, 2006]) during opposite NSG decadal phases. The distributions shown in Figure 4a indicate that three or more years of dry events are more likely to occur during the positive phase of the NSG (66%) than during the NSG negative phase (19%). Conversely, the chance of three or more years of rainy dry seasons during the NSG positive and negative phases is 30% and 77%, respectively.

The same calculation is performed for the HIST 145 and PIC 199 year long time series for a total of 136 and 190 ten year moving windows, respectively, applied to all 128 ensemble members that compose the HIST experiment and 42 for the PIC. The probability distributions of dry (Figure 4c) and wet (Figure 4d) dry seasons as a function of the decadal NSG index are also statistically different ($P < 0.01$) in both HIST and PIC simulations. These results combine the collective response of all models, and no attempt was made to select those that better represent the Amazon climate and SSTs teleconnections. Therefore, it should be expected that models more skillful in representing the NSG and western Amazon coupling would better solve the shifts in frequency of occurrence of dry and rainy dry seasons. Nevertheless, this first look at models' abilities to reproduce the NSG and western Amazon dry-season precipitation coupling, highlights the potential for decadal prediction of dry and wet events frequencies based on GCMs.

4. Discussion

A quantification of the relative importance of decadal fluctuations and long-term trends is essential when assessing past or future near-term climate change. This is especially relevant in regions, such as the western Amazon, where there is a marked decadal signal that can impose an acceleration or deceleration of trends calculated over periods shorter than the full decadal cycle. In comparison to this decadal variation, negative long-term trends explain a much lower portion of the hydroclimatic variables' total variance (<6%) over the period 1935–2012. The combination of trend and decadal component in its current phase likely contributed to the severity of the 2010 drought. Our results also reveal that the western Amazon decadal fluctuations vary closely with those of the north-south gradient of tropical and subtropical Atlantic SSTs, a process well reproduced in HIST and PIC model simulations. This suggests potential for decadal prediction based on GCMs. The repeated occurrence of dry and wet events also varies as a function of the decadal phase in the Atlantic NSG index, as it is more likely to observe three or more years of dry events during the positive NSG phase (66%) than during its negative phase (19%). The decadal component of the NSG index switched sign to become markedly positive in 2005. Persistence of the current positive NSG phase, as suggested by previous multiple-decades phase length, favors a continuation of above normal frequencies of western Amazon dry-season dry events in the coming decades. This has practical implications for fire occurrence, forest degradation, and consequently the global carbon cycle.

References

- ANA (2014), Monitoramento Hidrológico na Amazônia Ocidental em 2014, *Rep.*, 1–15 pp., Ministério do Meio Ambiente, Brasília.
- Aragão, L. E. O. C., and Y. E. Shimabukuro (2010), The incidence of fire in Amazonian Forests with implications for REDD, *Science*, 328(5983), 1275–1278.
- Ault, T. R., J. E. Cole, and S. S. George (2012), The amplitude of decadal to multidecadal variability in precipitation simulated by state-of-the-art climate models, *Geophys. Res. Lett.*, 39, L21705, doi:10.1029/2012GL053424.
- Booth, B. B. B., N. J. Dunstone, P. R. Halloran, T. Andrews, and N. Bellouin (2012), Aerosols implicated as a prime driver of twentieth-century North Atlantic climate variability, *Nature*, 484(7393), 228–232.
- Bosilovich, M. G., and J. D. Chern (2006), Simulation of water sources and precipitation recycling for the MacKenzie, Mississippi, and Amazon River basins, *J. Hydrometeorol.*, 7(3), 312–329.
- Brown, I. F., W. Schroeder, A. Setzer, M. de los Rios Maldonado, N. Pantoja, A. Duarte, and J. A. Marengo (2006), Monitoring fires in southwestern Amazonia Rain Forests, *Eos Trans. AGU*, 87(26), 253–264, doi:10.1029/2006EO260001.
- Chang, C. Y., J. C. H. Chiang, M. F. Wehner, A. R. Friedman, and R. Ruedy (2011), Sulfate aerosol control of tropical Atlantic climate over the twentieth century, *J. Clim.*, 24(10), 2540–2555.
- Chiang, J. C. H., C. Y. Chang, and M. F. Wehner (2013), Long-term behavior of the Atlantic interhemispheric SST gradient in the CMIP5 historical simulations, *J. Clim.*, 26(21), 8628–8640.
- Cook, B., N. Zeng, and J. H. Yoon (2012), Will Amazonia dry out? Magnitude and causes of change from IPCC climate model projections, *Earth Interact.*, 16, 1–27, doi:10.1175/2011EI398.1.
- Costa, M. H., and J. A. Foley (1999), Trends in the hydrologic cycle of the Amazon basin, *J. Geophys. Res.*, 104(D12), 14,189–14,198, doi:10.1029/1998JD200126.
- Cox, P. M., P. P. Harris, C. Huntingford, R. A. Betts, M. Collins, C. D. Jones, T. E. Jupp, J. A. Marengo, and C. A. Nobre (2008), Increasing risk of Amazonian drought due to decreasing aerosol pollution, *Nature*, 453(7192), 212–215.

Acknowledgments

Funding was provided by the United States Agency for International Development (grant agreement EEM-G-00-04-00010-00) and NSF-CNH-0909475. This research was part of the CGIAR research program on Forests, Trees, and Agroforestry. We acknowledge: the Global Precipitation Climatology Centre (GPCC) and the National Oceanic and Atmospheric Administration (NOAA) for providing the precipitation and SST data, accessible through the International Research Institute for Climate and Society (IRI) Data Library (<http://iridl.ldeo.columbia.edu/>); the Brazilian Water Agency (ANA) for providing the Rio Negro water level data <http://hidroweb.ana.gov.br/>; and the World Climate Research Programme (WCRP) for providing the CMIP5 GCM simulations (http://cmip-pcmdi.llnl.gov/cmip5/data_portal.html). We wish to thank Bradfield Lyon for helpful discussions.

The Editor thanks two anonymous reviewers for their assistance in evaluating this paper.

- da Costa, A. C. L., et al. (2010), Effect of 7 years of experimental drought on vegetation dynamics and biomass storage of an eastern Amazonian rainforest, *New Phytol.*, *187*(3), 579–591.
- DelSole, T., M. K. Tippett, and J. Shukla (2011), A significant component of unforced multidecadal variability in the recent acceleration of global warming, *J. Clim.*, *24*(3), 909–926.
- Dirmeyer, P. A., C. A. Schlosser, and K. L. Brubaker (2009), Precipitation, recycling, and land memory: An integrated analysis, *J. Hydrometeorol.*, *10*(1), 278–288.
- Ebisuzaki, W. (1997), A method to estimate the statistical significance of a correlation when the data are serially correlated, *J. Clim.*, *10*(9), 2147–2153.
- Eltahir, E. A. B., and R. L. Bras (1994), Precipitation recycling in the Amazon basin, *Q. J. R. Meteorol. Soc.*, *120*(518), 861–880.
- Enfield, D. B., A. M. Mestas-Nunez, and P. J. Trimble (2001), The Atlantic multidecadal oscillation and its relation to rainfall and river flows in the continental US, *Geophys. Res. Lett.*, *28*(10), 2077–2080, doi:10.1029/2000GL012745.
- Fernandes, K., et al. (2011), North tropical Atlantic influence on western Amazon fire season variability, *Geophys. Res. Lett.*, *38*, L12701, doi:10.1029/2011GL047392.
- Folland, C., T. Palmer, and D. Parker (1986), Sahel rainfall and worldwide sea temperatures, 1901–85, *Nature*, *320*(6063), 602–607.
- Fu, R., R. E. Dickinson, M. X. Chen, and H. Wang (2001), How do tropical sea surface temperatures influence the seasonal distribution of precipitation in the equatorial Amazon?, *J. Clim.*, *14*(20), 4003–4026.
- Fu, R., et al. (2013), Increased dry-season length over southern Amazonia in recent decades and its implication for future climate projection, *Proc. Natl. Acad. Sci. U.S.A.*, *110*(45), 18,110–18,115.
- Giannini, A., R. Saravanan, and P. Chang (2003), Oceanic forcing of Sahel rainfall on interannual to interdecadal time scales, *Science*, *302*(5647), 1027–1030.
- Giannini, A., S. Salack, T. Lodoun, A. Ali, A. T. Gaye, and O. Ndiaye (2013), A unifying view of climate change in the Sahel linking intra-seasonal, interannual and longer time scales, *Environ. Res. Lett.*, *8*(2), 024010.
- Good, P., J. A. Lowe, M. Collins, and W. Moufouma-Okia (2008), An objective tropical Atlantic sea surface temperature gradient index for studies of south Amazon dry-season climate variability and change, *Philos. Trans. R. Soc. B*, *363*(1498), 1761–1766.
- Good, P., J. A. Lowe, and D. P. Rowell (2009), Understanding uncertainty in future projections for the tropical Atlantic: Relationships with the unforced climate, *Clim. Dyn.*, *32*(2–3), 205–218.
- Greene, A. M., L. Goddard, and R. Cousin (2011), Web tool deconstructs variability in twentieth-century climate, *Eos Trans. AGU*, *92*(45), 397–398, doi:10.1029/2011EO450001.
- Hastenrath, S. (1990), Decadal-scale changes of the circulation in the tropical Atlantic sector associated with Sahel drought, *Int. J. Climatol.*, *10*(5), 459–472.
- Joetzer, E., H. Douville, C. Delire, and P. Ciais (2013), Present-day and future Amazonian precipitation in global climate models: CMIP5 versus CMIP3, *Clim. Dyn.*, *41*(11–12), 2921–2936.
- Kayano, M. T., C. P. de Oliveira, and R. V. Andreoli (2009), Interannual relations between South American rainfall and tropical sea surface temperature anomalies before and after 1976, *Int. J. Climatol.*, *29*(10), 1439–1448.
- Knutti, R., and J. Sedlacek (2013), Robustness and uncertainties in the new CMIP5 climate model projections, *Nat. Clim. Change*, *3*(4), 369–373.
- Kossin, J. P., and D. J. Vimont (2007), A more general framework for understanding Atlantic hurricane variability and trends, *Bull. Am. Meteorol. Soc.*, *88*(11), 1767–1781.
- Latif, M., M. Collins, H. Pohlmann, and N. Keenlyside (2006), A review of predictability studies of Atlantic sector climate on decadal time scales, *J. Clim.*, *19*(23), 5971–5987.
- Li, W. H., and R. Fu (2004), Transition of the large-scale atmospheric and land surface conditions from the dry to the wet season over Amazonia as diagnosed by the ECMWF re-analysis, *J. Clim.*, *17*(13), 2637–2651.
- Li, W. H., R. Fu, R. I. N. Juarez, and K. Fernandes (2008), Observed change of the standardized precipitation index, its potential cause and implications to future climate change in the Amazon region, *Philos. Trans. R. Soc. B*, *363*(1498), 1767–1772.
- Malhi, Y., and J. Wright (2004), Spatial patterns and recent trends in the climate of tropical rainforest regions, *Philos. Trans. R. Soc. London B*, *359*(1443), 311–329.
- Marengo, J. A. (2009), Long-term trends and cycles in the hydrometeorology of the Amazon basin since the late 1920s, *Hydrol. Processes*, *23*(22), 3236–3244.
- Marengo, J. A., J. Tomasella, L. M. Alves, W. R. Soares, and D. A. Rodriguez (2011), The drought of 2010 in the context of historical droughts in the Amazon region, *Geophys. Res. Lett.*, *38*, L12703, doi:10.1029/2011GL047436.
- Martin, E. R., C. Thorncroft, and B. B. Booth (2014), The multidecadal Atlantic SST-Sahel Rainfall Teleconnection in CMIP5 simulations, *J. Clim.*, *27*(2), 784–806.
- McKee, T. B., N. J. Doesken, and J. Kleist (1993), The relationship of drought frequency and duration to time scales, in *8th Conference on Applied Climatology*, pp. 179–186, Am. Meteorol. Soc., Anaheim, Calif., 17–23 Jan.
- Meehl, G., T. Stocker, W. Collins, P. Friedlingstein, A. Gaye, J. Gregory, A. Kitoh, R. Knutti, J. Murphy, and A. Noda (2007), Global climate projections, in *Climate Change 2007: The Physical Science Basis. Contribution of Working Group I to the Fourth Assessment Report of the Intergovernmental Panel on Climate Change*, edited by S. Solomon et al., chap. 10, pp. 747–845, Cambridge Univ. Press, Cambridge, U. K., and New York.
- Orlowsky, B., and S. I. Seneviratne (2013), Elusive drought: Uncertainty in observed trends and short- and long-term CMIP5 projections, *Hydrol. Earth Syst. Sci.*, *17*(5), 1765–1781.
- Parsons, L. A., J. J. Yin, J. T. Overpeck, R. J. Stouffer, and S. Malyshev (2014), Influence of the Atlantic meridional overturning circulation on the monsoon rainfall and carbon balance of the American tropics, *Geophys. Res. Lett.*, *41*, 146–151, doi:10.1002/2013GL058454.
- Ropelewski, C. F., and M. S. Halpert (1987), Global and regional scale precipitation patterns associated with the El-Niño Southern Oscillation, *Mon. Weather Rev.*, *115*(8), 1606–1626.
- Saatchi, S., S. Asefi-Najafabady, Y. Malhi, L. E. Aragão, L. O. Anderson, R. B. Myneni, and R. Nemani (2013), Persistent effects of a severe drought on Amazonian forest canopy, *Proc. Natl. Acad. Sci. U.S.A.*, *110*(2), 565–570.
- Salati, E., and P. B. Vose (1984), Amazon basin: A system in equilibrium, *Science*, *225*(4658), 129–138.
- Schamm, K., M. Ziese, A. Becker, P. Finger, A. Meyer-Christoffer, U. Schneider, M. Schröder, and P. Stender (2014), Global gridded precipitation over land: A description of the new GPCC First Guess Daily product, *Earth Syst. Sci. Data*, *6*(1), 49–60.
- Schneider, U., A. Becker, P. Finger, A. Meyer-Christoffer, M. Ziese, and B. Rudolf (2014), GPCC's new land surface precipitation climatology based on quality-controlled in situ data and its role in quantifying the global water cycle, *Theor. Appl. Climatol.*, *115*(1–2), 15–40.
- Smith, T. M., R. W. Reynolds, T. C. Peterson, and J. Lawrimore (2008), Improvements to NOAA's historical merged land-ocean surface temperature analysis (1880–2006), *J. Clim.*, *21*(10), 2283–2296.

- Stocker, T. F., D. Qin, G. K. Plattner, M. Tignor, S. K. Allen, J. Boschung, A. Nauels, Y. Xia, V. Bex, and P. M. Midgley (2013), *Climate Change 2013: The Physical Science Basis. Contribution of Working Group I to the Fifth Assessment Report of the Intergovernmental Panel on Climate Change*, 1535 pp., Cambridge Univ. Press, Cambridge, U. K., and New York.
- Svoboda, M., M. Hayes, and D. Wood (2012), *Standardized Precipitation Index User Guide*, WMO-No. 1090, World Meteorol. Organ., Geneva, Switzerland.
- Taylor, K. E., R. J. Stouffer, and G. A. Meehl (2012), An overview of CMIP5 and the experiment design, *Bull. Am. Meteorol. Soc.*, *93*(4), 485–498.
- Terray, L. (2012), Evidence for multiple drivers of North Atlantic multi-decadal climate variability, *Geophys. Res. Lett.*, *39*, L19712, doi:10.1029/2012GL053046.
- Ting, M. F., Y. Kushnir, R. Seager, and C. H. Li (2009), Forced and internal twentieth-century SST trends in the North Atlantic, *J. Clim.*, *22*(6), 1469–1481.
- Ting, M. F., Y. Kushnir, R. Seager, and C. H. Li (2011), Robust features of Atlantic multi-decadal variability and its climate impacts, *Geophys. Res. Lett.*, *38*, L17705, doi:10.1029/2011GL048712.
- van der Ent, R. J., H. H. G. Savenije, B. Schaefli, and S. C. Steele-Dunne (2010), Origin and fate of atmospheric moisture over continents, *Water Resour. Res.*, *46*, W09525, doi:10.1029/2010WR009127.
- Villar, J. C. E., J. Ronchail, J. L. Guyot, G. Cochonneau, F. Naziano, W. Lavado, E. De Oliveira, R. Pombosa, and P. Vauchel (2009), Spatio-temporal rainfall variability in the Amazon basin countries (Brazil, Peru, Bolivia, Colombia, and Ecuador), *Int. J. Climatol.*, *29*(11), 1574–1594.
- Wang, C. Z. (2002), Atlantic climate variability and its associated atmospheric circulation cells, *J. Clim.*, *15*(13), 1516–1536.
- Wilks, D. S. (2006), *Statistical Methods in the Atmospheric Sciences*, *Int. Geophys. Ser.*, vol. 91, 2nd ed., Elsevier, Oxford, U. K.
- Yoon, J. H., and N. Zeng (2010), An Atlantic influence on Amazon rainfall, *Clim. Dyn.*, *34*(2–3), 249–264.
- Zeng, N. (1999), Seasonal cycle and interannual variability in the Amazon hydrologic cycle, *J. Geophys. Res.*, *104*(D8), 9097–9106, doi:10.1029/1998JD200088.
- Zhang, R., et al. (2013), Have aerosols caused the observed Atlantic multidecadal variability?, *J. Atmos. Sci.*, *70*(4), 1135–1144.